Dalton Transactions

ROYAL SOCIETY OF CHEMISTRY

PERSPECTIVE

Cite this: *Dalton Trans.*, 2020, **49**, 10295

A practical guide to calculate the isosteric heat/enthalpy of adsorption *via* adsorption isotherms in metal–organic frameworks, MOFs†‡

Alexander Nuhnen and Christoph Janiak *

Porous materials such as MOFs are interesting candidates for gas separation and storage. An important parameter to gain deeper insights to the adsorption process of an adsorptive on an adsorbent is the isosteric enthalpy of adsorption, ΔH_{ads} which is defined as the heat to be released/required when an adsorptive binds to/detaches from the solid surface of an adsorbent. Two or three adsorption isotherms at different but close temperatures with $\Delta T \leq 20$ K for two and $\Delta T \approx 10$ K for three isotherms are the basis to derive the isosteric enthalpy of adsorption through the Clausius–Clapeyron approach or the virial analysis. This Perspective presents the procedure of the common (dual-site) Freundlich–Langmuir fit/Clausius–Clapeyron approach and the virial fit of the isotherms with usable Excel sheets and Origin files for the subsequent derivation of ΔH_{ads}. Exemplary adsorption isotherms of CO_2, SO_2 and H_2 at two temperatures on MOFs are analyzed. The detailed computational description and comparison of the Clausius–Clapeyron approach and the virial analysis to determine ΔH_{ads} outlines the limitations of the two methods with respect to the available experimental data, especially at low pressure/low uptake values. It is emphasized that no extrapolation beyond the experimental data range should be done. The quality of the important and underlying isotherm fits must be checked and ensured with logarithmic-scale n/p isotherm plots for the (dual-site) Freundlich–Langmuir fit in the low-pressure region and through low standard deviations for the coefficients in the virial analysis.

Received 18th May 2020,
Accepted 6th July 2020

DOI: 10.1039/d0dt01784a

rsc.li/dalton

Introduction

Gas sorption for storage and separation is of continuous interest with porous materials, such as activated carbon, zeolites, silica gel, metal–organic frameworks (MOFs) *etc*. At the moment, MOFs, which are potentially porous three-dimensional coordination polymers,[1] appear to receive the highest attention for such gas sorption applications, as they feature a high functional and composition diversity.[2] MOFs are built from metal ions or metal clusters, connected by multidentate organic ligands and can be tuned in regards to their physiochemical properties depending on their organic and inorganic building blocks.[3] Over the last two decades plenty of studies about gas separation and storage in MOFs have been published.[4,5]

Of interest for gas sorption with MOFs are, *e.g.*, carbon capture and storage (CCS) technologies.[6,7] Furthermore, MOFs with high hydrogen uptake are envisioned for energy storage and as carrier in mobile applications,[8,9] in order to achieve a higher volumetric energy density, which is otherwise only accessible under high pressures (up to 700 bar) or cryogenically (cooled to 20 K). By physisorption of supercritical gases, such as dihydrogen in a porous material a liquid-like adsorbate phase (with higher than gas density) is formed. For practical use at operating conditions of 1.5 to 30 bar at 298 K lightweight materials with high adsorption capacities and binding enthalpies of about −15 to −20 kJ mol^{-1} are required.[10,11] Higher H_2 binding enthalpies are achieved by chemisorption of H_2 as in metal hydrides or other materials which store hydrogen through chemical bond formation; there the release is slow and requires heating.[12] Besides, the sorption of CO_2 and H_2, also CH_4 separation and storage draws interest[13] and an effective capture of harmful gases such as SO_2 and NO_x is of growing importance.[14]

In the chemical industry the separation of gas mixtures by pressure swing or thermal swing adsorption at a surface is an

Institut für Anorganische Chemie und Strukturchemie, Heinrich-Heine-Universität Düsseldorf, D-40204 Düsseldorf, Germany. E-mail: janiak@hhu.de

† In order not to interrupt the flow of reading we have added a glossary for sorption specific terms as Appendix.

‡ Electronic supplementary information (ESI) available: Details for Clausius–Clapeyron and virial equation, Freundlich–Langmuir fit of *n vs. p* isotherms, MOF structures, SO_2 adsorption isotherms of NH_2-MIL-125(Ti) at 273 K and 293 K, virial analysis for SO_2 isotherms of NH_2-MIL-125(Ti) at 273 K and 293 K with a larger number of a_i and b_i fit parameters, enthalpy of adsorption for CO_2 on MIL-100(Cr), workable Excel and ORIGIN files with data sheets. See DOI: 10.1039/d0dt01784a

established process.[15] The surface is part of the adsorbent; the adsorbed species become the adsorbate. For the separation of two species from a gaseous mixture, these two species (assuming the same unrestricted accessibility to the surface) must have different interaction energies with the surface, so that one is preferentially adsorbed over the other. The actual amount adsorbed of adsorbate at a given mass of adsorbent depends on the relative pressure and the temperature together with the adsorbate–adsorbent interaction energy.

We note that for this interaction energy the terms "heat of adsorption", "isosteric heat of adsorption" both with the symbol Q_{st} and "(isosteric) enthalpy of adsorption, ΔH_{ads}" appear to be used indiscriminately. In most of the MOF literature it is not clearly distinguished between the two expressions of ΔH_{ads} and Q_{st} and they appear to be used interchangeably to describe binding energies. The use of the term "isosteric heat of adsorption", Q_{st} is discouraged since it does not correspond to any well-defined thermodynamic change of state. It has been suggested that the term "isosteric heat" is preferably replaced by the term "isosteric enthalpy of adsorption, ΔH_{ads}".[16] Q_{st} is a positive quantity and for an adsorption process the enthalpy of adsorption, ΔH_{ads} has to be negative, in short $\Delta H_{ads} = -Q_{st}$.[17,18] The isosteric enthalpy of adsorption, ΔH_{ads} is defined as the heat which is released when an adsorptive binds to a surface.[19] The higher the magnitude of (*i.e.*, more negative) the adsorption enthalpy for an adsorbate–adsorbent pair, the more species will be adsorbed at a given pressure and temperature. The enthalpy of adsorption is released during the adsorption process ($\Delta H_{ads} < 0$ kJ mol^{-1}) and in the case of physisorption (without activation barrier), is the reverse of the enthalpy of desorption, ΔH_{des}, which is required for the reverse process of desorption ($\Delta H_{ads} = -\Delta H_{des}$). For chemisorption the situation is more complicated as the chemical adsorption is characterized by large interaction potentials, leading to high enthalpies of adsorption in the range of chemical bonds. The process of chemisorption is also associated with activation energies as for most chemical reactions.

Generally, adsorption materials should meet several requirements to be suitable for a sorption application, such as high selectivity, low regeneration energies and high working capacity.[20] Consequently, the enthalpy of adsorption is an important parameter in adsorption processes and is further used to gain deeper insights into the adsorbate–adsorbent interactions. Since ΔH_{ads} depends on the strength of the interaction for an adsorbate–adsorbent pair, it is possible to classify the interactions of the adsorbed species with the adsorbent, *e.g.* if weak physisorption or strong chemisorption is present. In the same way, ΔH_{ads} can be used to determine the regeneration energies for the desorption of the adsorbate. Regeneration energies are especially important for pressure swing experiments, as the energy required for desorption depends on the binding strength.[21]

Approaches to determine ΔH_{ads} can initially be divided into two types, experiment-based calculations and molecular simulations. The simulated enthalpies of adsorption in the latter are mostly based on isotherms obtained by grand canonical Monte Carlo simulations (GCMS) and calculated *via* the ensemble fluctuation approach.[22] The experimental procedures can be divided into a direct and indirect approach. In the direct approach, using a calorimetric–volumetric system, it is possible to directly measure the released heat during the adsorption with a calorimeter.[23] Since these systems are very complex and costly, only very few studies use the direct method to determine ΔH_{ads}.[6] The by far most common way to determine the isosteric enthalpy of adsorption as a function of the amount adsorbed (loading) is *via* the indirect approach using adsorption isotherms. The adsorbate–adsorbent interaction energy is typically assessed indirectly from at least two adsorption isotherms obtained at close but different temperatures (T_1, T_2) with $\Delta T \approx$ 10–20 K. We recommend to use, if possible, three adsorption isotherms with ΔT = 10 K to obtain isosteric enthalpies and in order to increase statistical significance and to be able to report error values (see Excel sheet Ex0, ESI‡ how to calculate errors by the standard error of the linear regression in the plot of ln p *vs.* $1/T$). The calculation of error values is a check on the reported parameters, since large error values indicate either a problem during data collection or that the data has not been well-modeled. Since the isosteric enthalpy of adsorption is temperature dependent, applying a large temperature range (ΔT > 20 K) between the adsorption isotherms will artificially introduce errors into the calculated value. Therefore, we strongly recommend to use at the most a 20 K step (and not 25 or 30 K) for isotherms measured in the 273–298 K range if only two temperatures are compared to mitigate the impact of the inherent error.

Adsorption isotherms are most typically obtained through volumetric gas sorption measurements. For gases such as CO_2, CH_4 and SO_2 isotherms are usually measured at around standard conditions, for example at 273 K and 293 K from 0 to 1 bar (0–101.3 kPa). This is due to the relative high uptake for many MOF materials even at elevated temperatures for these gases, compared to their respective boiling point. H_2 isotherms are mostly collected at 77 K and 87 K, as the overall uptake at higher temperatures is insufficient. These adsorption isotherms form the basis for either the Clausius–Clapeyron approach or the virial analysis to derive the isosteric enthalpy (ΔH_{ads}) or heat (Q_{st}), respectively, of adsorption.

For the Clausius–Clapeyron approach the two adsorption isotherms should be fitted with the same continuous function, *e.g.* a Langmuir, dual-site Langmuir, Toth, Sips, Jovanovic, Dubinin–Radushkevic, Freundlich–Langmuir or other fit.[24a] The Langmuir isotherm is based on the model of monolayer adsorption on a solid (see Glossary for details) and is often used to fit for Type-I gas uptake isotherms on microporous solids with complete pore filling. Especially for bimodal pore distributions or different binding sites of the adsorbent a dual-site approach is beneficial. For adsorption isotherms in the state before the actual pore-filling regime, empirical models like Toth or Freundlich are commonly utilized to describe the adsorbate–adsorbent interactions.[24b] After the fitting procedure the isotherms are evaluated for pressure

(p)–loading (n) data pairs with the same loading n at each temperature. This is known as the "isosteric" method, based on the use of the Clausius–Clapeyron equation (eqn (1))[25] (see section S1, ESI‡).

$$\Delta H_{ads}(n) = -R \cdot \ln\left(\frac{p_2}{p_1}\right) \frac{T_1 \cdot T_2}{(T_2 - T_1)} \quad (1)$$

R = ideal gas constant.

The Clausius–Clapeyron equation relates the adsorption heat effects to the temperature dependence of the adsorption isotherm. There are two approximations made in deriving the Clausius–Clapeyron equation, (i) a negligible molar volume of the adsorbed phase and (ii) ideal gas behavior of the gaseous phase (see section S1, ESI‡). Thus, the ΔH_{ads} values from this approach can differ from the direct experimental data, especially at higher loadings (*vide infra*).[25]

For the virial analysis, the isotherms are fitted according to the virial-type equation (eqn (2)), which expresses the pressure p as a function of loading n of a gas (see section S2, ESI‡). Especially for highly polarized gases such as CO_2 and SO_2 the virial analysis has been used for calculating enthalpies of adsorption.[26,27]

$$p = n \cdot \exp\left(\sum_{i=0}^{m} C_i n^i\right) \quad (2)$$

In eqn (2) C_0 is a constant for the adsorbate–adsorbent interaction, C_1, C_2 *etc*. are constants for the double, triple *etc*. interactions in the adsorbent field. The constants C_i depend on temperature and the heat of adsorption Q_{st} (not to be mistaken as the enthalpy of adsorption, since $\Delta H_{ads} = -Q_{st}$) is given as (eqn (3))[28]

$$Q_{st}(n) = \left(\sum_{i=0}^{m} \frac{dC_i}{dT} RT^2 n^i\right) \quad (3)$$

Note that $\Delta H_{ads}(n)$ or $Q_{st}(n)$ is typically given only as ΔH_{ads} or Q_{st} in the literature, but definitely varies with loading. The amount adsorbed (n), *i.e.*, the surface coverage or loading of an adsorbent is important for ΔH_{ads} or Q_{st} calculations. Most materials feature different adsorption sites with different surfaces energies and thus ΔH_{ads} or Q_{st} depends on the surface coverage of the adsorbent. In return, it is possible to illustrate the energetic heterogeneity, that is, elucidate different adsorption sites of a solid surface when ΔH_{ads} or Q_{st} is plotted against the adsorbed amount n.

In the literature most papers dealing with enthalpy of adsorption from the Clausius–Clapeyron or virial approach essentially state the basic formula and only occasionally also give further information, such as the applied fit of the isotherms. Programs that are implemented with the automatic gas sorption measurement devices can provide ΔH_{ads} plots based on two adsorption isotherms at two temperatures. However, the used method may not be apparent from the manual and software and not necessarily available from the company. Thus, the determination of ΔH_{ads} becomes a black-box method, the underlying principle and pitfalls may no longer be evident.

In this work, we focus on the material class of MOFs, which are currently investigated by researchers coming from disciplines such as organic chemistry, crystal engineering, coordination chemistry, synthesis, crystallography, solid-state (zeolite) chemistry and theoretical chemistry. Structural details for all MOF materials included in this study can be found in the ESI.‡ For example, to improve the above noted H_2 storage by physisorption in MOFs, current research aims to increase the enthalpy of adsorption. At present $\Delta H_{ads}(H_2)$ in most MOFs is typically −5 to −7 kJ mol^{-1}, much lower than the targeted −15 to −20 kJ mol^{-1}. Thus, in such work the determination of the enthalpy of adsorption is fundamental.[9,10,12]

New researchers entering the field of porous materials and especially MOFs may benefit from a detailed description of the various methods to determine the isosteric enthalpy of adsorption, including the weaknesses, strengths and the procedure of isotherm fitting by the common methods *e.g.* Freundlich–Langmuir and virial analysis (*vide infra*). The specific goal of this Perspective is not only to describe these methods, but to provide usable Excel data sheets with implemented formulae, where the data from gas sorption isotherms can be pasted into, in order to calculate the isosteric enthalpy of adsorption (see section S3, ESI‡ for details).

Clausius–Clapeyron approach

Via Freundlich–Langmuir fit of *n vs. p* isotherms

The two isotherms at two temperatures must be fitted with the same model. At the mentioned conditions most MOFs will exhibit a Freundlich–Langmuir-type isotherm, which can be fitted with the following Freundlich–Langmuir eqn (4):

$$n = \frac{a \cdot b \cdot p^c}{1 + b \cdot p^c} \quad (4)$$

where n is the amount adsorbed (the loading) in mmol g^{-1}, p the pressure in kPa, a is the maximal loading in mmol g^{-1}, b the affinity constant (1/kPa^c) and c the heterogeneity exponent [the product of $b{\cdot}p^c$ must be dimension-less. We note that in the literature eqn (4) also takes the form with $(b{\cdot}p)^c$, then b would have simply the unit 1/kPa].

In Fig. 1 an example for the Freundlich–Langmuir fit of CO_2 adsorption isotherms for MIL-160 at 273 K and 293 K is depicted.

A detailed description how to create fitting curves in the program Origin[30] is given in section S3 and in the pdf slides in the ESI.‡ Afterwards one has to rearrange the Freundlich–Langmuir equation as follows:

$$p(n) = \sqrt[c]{\frac{n}{a \cdot b - n \cdot b}} \quad (5)$$

Now one can calculate the pressures p_1 and p_2 for both temperatures T_1 and T_2, respectively at the same loading n by plugging in the respective values for a, b and c derived from

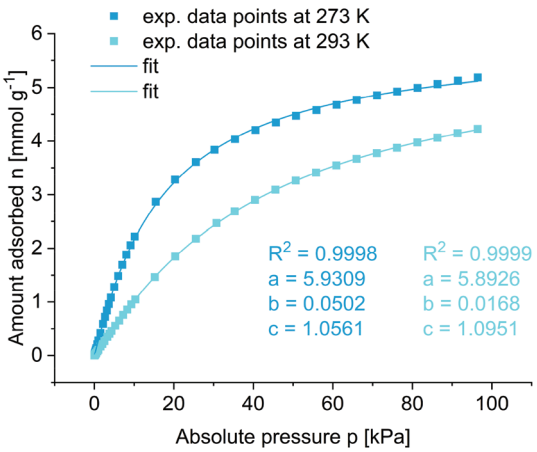

Fig. 1 Freundlich–Langmuir fit for CO_2 adsorption isotherms on MIL-160 at 273 K and 293 K. See ESI‡ for structure details of MIL-160. Isotherm data taken from ref. 29.

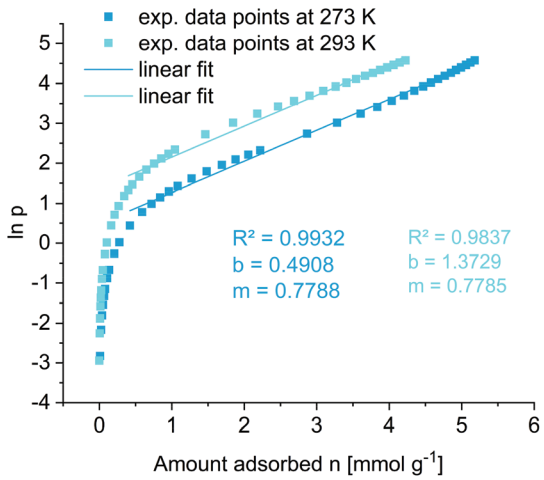

Fig. 2 '$\ln p$ against n' plot from the CO_2 adsorption isotherms on MIL-160 at 273 K and 293 K (*cf.* Fig. 1) with a linear fit approximation in the region of $0.4 < n <$ maximum uptake. See ESI‡ for structure details of MIL-160. Isotherm data taken from ref. 29.

the Freundlich–Langmuir fit from Fig. 1. With this approach one can compare the pressures at isosteric conditions, that is at the same uptake of the adsorbate. The fitting routine leads to a continuous sequence of $n|p$ data pairs.

One may wonder why the two $n|p_1$ and $n|p_2$ data pairs could not be directly taken from the experimental data points of the two isotherms: unless both isotherms were measured with a very large number of data points (concomitant with small pressure intervals) there will not be both pressure values p_1 and p_2 available for the same n. An interpolation or estimation of p values for a given n value is not practical and not accurate enough. Thus, the fit serves essentially to provide a continuum of $n|p_1$ and $n|p_2$ data pairs or rather $n|p_1|p_2$ data triples.

To get the most reliable data for the isosteric enthalpy of adsorption one should not extrapolate beyond the measured data points, that is to lower or higher uptake and pressure. Such tempting extrapolation should especially not be done to uptakes in the low-pressure region if these data points could not be measured due to limitations in the instrument setup. Note, that low-pressure regimes ($p/p_0 < 0.001$, or $p_{absolute} <$ 1.0 mbar) can only be measured if the gas sorption analyzer is fitted with the necessary low-pressure 1 Torr transducer (pressure sensor) and if the instrument is equipped with a turbomolecular pump to provide a low starting pressure.

Therefore, only pressures in the range of the measured gas uptake for both isotherms can and should be calculated. The calculation is provided in the Excel sheet named Ex1 (ESI‡).

Via straight-line fit of $\ln p$ *vs.* n isotherms

The $n|p$ data pairs in the measured adsorption isotherms can be transformed into $n|\ln p$ data pairs (section S3.6, ESI‡). We note that in the literature the adsorption isotherms in an '$\ln p$ against n' plot are then fitted with a straight line ($\ln p = m{\cdot}n + b$) in a suitable region (Fig. 2, section S3.7 and S3.8, ESI‡).[31]

This straight-line or '$\ln p$ *vs.* n'-fit approach is mathematically simpler as the Freundlich–Langmuir fit.

From the '$\ln p$ *vs.* n'-plot in Fig. 2 it is, however, evident that there are only sections where $\ln p$ against n can be approximated by a straight line. For the example in Fig. 2, this is the case from $0.001 < n < 0.1$ or $0.4 < n <$ maximum uptake. The straight-line approximation at the two temperatures then serves to provide a continuum of $n|\ln p_1|\ln p_2$ data triples, yet, only over a limited uptake region, compared with the Freundlich–Langmuir fit.

Only for gases with low affinity to the adsorbent the function of $\ln p$ against n becomes fairly linear over a wider uptake region. However, for most gases adsorbed on MOF materials this straight-line approximation of $\ln p$ *versus* n is not practical, because of stronger interactions between adsorbate and adsorbent, hence the isotherm has to be fitted by the Freundlich–Langmuir model as described above. For the example in Fig. 2, we use the region of $0.4 < n <$ maximum uptake where, in a first approximation, the two isotherms were fitted by a linear function and then used to derive $\Delta H_{ads}(n)$.

$\Delta H_{ads}(n)$ from $\ln p$ against $1/T$

$\Delta H_{ads}(n)$ can be calculated from the derived pressures (p_1, p_2 or $\ln p_1$, $\ln p_2$) at equal loadings (n). Using the $n|p_1|p_2$ or $n|\ln p_1|\ln p_2$ data triples from either the Freundlich–Langmuir or the straight-line fits, respectively, the isosteric enthalpy of adsorption is then calculated by plotting $\ln p$ against $1/T$ for the isosteric adsorptions, that is, for equal n at the two temperatures (Fig. 3). The slope m of the straight line with the two data points at $\ln p_1|1/T_1$ and $\ln p_2|1/T_2$ at equal loading n will give $\Delta H_{ads}(n)$ according to eqn (6).[28] For computational details of this calculation approach see section S3.5 and Excel sheet Ex1 (ESI‡).

For didactic purpose, we plotted $\ln p$ against $1/T$ for 10 loadings n in Fig. 3. For computational details of this simplistic

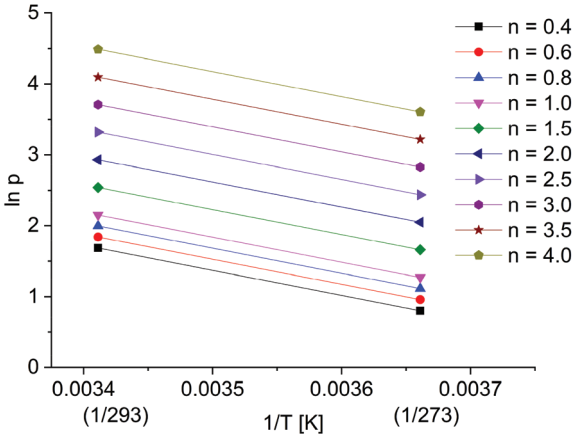

Fig. 3 Isosteric ln p against $1/T$ plot for T_1 = 273 K and T_2 = 293 K for 10 different loadings n (in mmol g^{-1}) to illustrate the determination of $\Delta H_{ads}(n)$ from the slopes ($m = \Delta H_{ads}(n)/R$) of the straight lines (R = universal gas constant) (see also section S1, ESI‡).

calculation approach see section S3.9 and Excel sheet Ex2 (ESI‡).

$$\Delta H_{ads}(n) = R \cdot m \quad (6)$$

The isosteric enthalpy of adsorption, $\Delta H_{ads}(n)$ from a Freundlich–Langmuir fit of the isotherms and from the straight-line-fit of a '$\ln p$ against n' plot in the region of $0.4 < n <$ maximum uptake is compared in Fig. 4. Both fit methods give similar results for the isosteric enthalpy of adsorption at high amounts adsorbed, but not for the low-uptake region. The '$\ln p$ *vs.* n plot' method underestimates $\Delta H_{ads}(n)$ significantly. The slopes of the two straight lines in Fig. 2 were essentially equal which also leads to the special case of a constant ΔH_{ads} that is independent from loading.

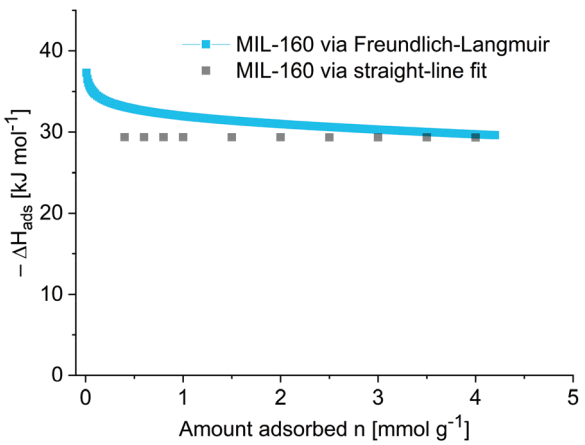

Fig. 4 Isosteric enthalpy of adsorption of CO_2 for MIL-160. The blue curve shows $\Delta H_{ads}(n)$ from a Freundlich–Langmuir fit of the isotherms with n_{min} = 0.01 mmol g^{-1} (Fig. 1). The grey data points represent $\Delta H_{ads}(n)$ derived from the straight-line fit of a '$\ln p$ against n' plot in the region of $0.4 < n <$ maximum uptake (Fig. 2 and 3).

ΔH_{ads} describes the strength of the binding energy between adsorbate and adsorbent. It is expected that the value changes with the uptake during the adsorption process. A high enthalpy of adsorption is reasoned by a strong affinity between adsorbate and adsorbent. Typically, the adsorption sites with the highest affinity to the adsorbate species are occupied at low pressure. These adsorption sites correlate with higher (negative) ΔH_{ads} values for very low loadings, as is evident in Fig. 4. The interaction energy for the "first few molecules" is generally called enthalpy of adsorption at zero coverage ($n \rightarrow 0$, ΔH^0_{ads}). In the literature often only the value for zero coverage ΔH^0_{ads} is given and discussed. This value of ΔH^0_{ads} can differ distinctly from ΔH_{ads} for the bulk adsorption. Also, the values for ΔH^0_{ads} are often questionable, since mostly not enough experimental data points are collected at such low loadings or they are even just extrapolated through the fitting procedure. After the occupation of the preferred binding sites the enthalpy of adsorption usually declines with increasing uptake. Upon pore filling ΔH_{ads} eventually approaches the interaction energy of the adsorptive molecules, that is, the enthalpy of liquefaction or evaporation, which is 17 kJ mol^{-1} for CO_2. In Fig. 4 ΔH_{ads} is still far from this 17 kJ mol^{-1} because the adsorption isotherms did not reach the pore-filling regime at the highest measured pressure of 100 kPa (Fig. 1).

Careful evaluation of the performance of a porous material should consider the enthalpy of adsorption over the entire adsorption range (not just at zero coverage). At zero to low coverage the magnitude of the isosteric enthalpy of adsorption is largely a function of the binding strength of the strongest binding sites within the material. These (few) high energy sites are, however, rapidly saturated already at low uptake. For the uptake to continue also the remaining sites must have an interaction energy which is above the enthalpy of liquefaction or evaporation.

Furthermore, to increase the significance of the values for the isosteric enthalpy of adsorption, we recommend to use three temperatures to determine ΔH_{ads} and to be able to include a standard deviation for every given value. As the temperature interval to derive ΔH_{ads} should not exceed 20 K we measured a third CO_2 adsorption isotherm on MIL-160 at 283 K and applied the same Freundlich–Langmuir fit as depicted earlier (Fig. S4‡). Afterwards we used the linear regression in the plot of $\ln p$ *vs.* $1/T$ for all three temperatures to estimate ΔH_{ads} and the associate error values (see Excel sheet Ex0, ESI‡).

Fig. 5 displays the isosteric enthalpy of adsorption derived from three temperatures with error values. Compared to Fig. 4 (ΔH_{ads} of MIL-160 calculated from two CO_2 adsorption isotherms at 273 K and 293 K) the absolute values for ΔH_{ads} derived from the linear regression of the plot of $\ln p$ *vs.* $1/T$ (T = 273, 283 and 293 K) in Fig. 5 remain similar. The error value for the lowest uptake point at n_{min} = 0.01 mmol g^{-1} is given with 0.40 kJ mol^{-1} and at first decreases with increasing uptake. After a minimum for the error of 0.01 kJ mol^{-1} at n = 0.05 mmol g^{-1} the error values gradually increase up to 2.7 kJ mol^{-1} at the highest loading of n = 4.2 mmol g^{-1}. In general,

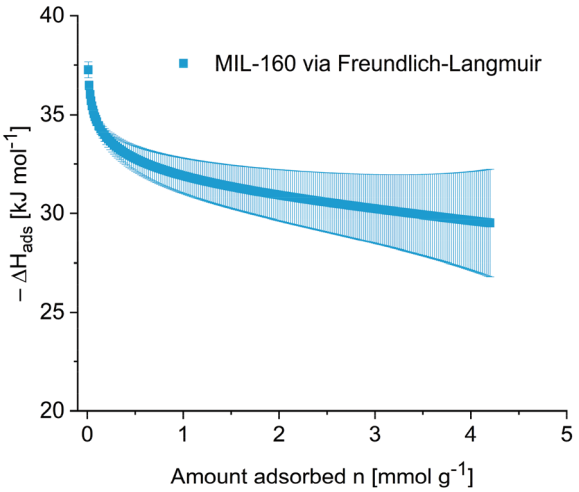

Fig. 5 Isosteric enthalpy of adsorption of CO_2 for MIL-160, derived from three temperatures (273, 283 and 293 K) with standard deviation. Calculated *via* Freundlich–Langmuir fitting of the isotherms with n_{min} = 0.01 mmol g^{-1} (Fig. S4, ESI‡). The curve is very similar to the curve in Fig. 4 (derived from two temperature). In order to visualize the error bars, the $-\Delta H_{ads}$ (*y*-) scale ranges here only from 20 to 40 kJ mol^{-1}.

error values serve as a check on the derived parameters, with large error values indicating a problem during data modelling or data collection.

Virial analysis

For the virial fit the two isotherms measured at two different temperatures are brought into an ln *p vs. n* form (Fig. 6, *cf.* Fig. 2). Eqn (7) is then used to fit both isotherms simultaneously, that is with the same(!) fitting parameters a_i and b_j. It is crucial to use the same fitting parameters for both isotherms, hence to compromise in the optimization of the simultaneous fit of both isotherms. Thereby it is important to use as few fitting parameters a_i and b_j as possible.

$$\ln p = \ln n + \frac{1}{T}\sum_{i=0}^{m} a_i n^i + \sum_{i=0}^{m} b_i n^i \qquad (7)$$

In eqn (7), p is the pressure in kPa, n is the of total amount adsorbed in mmol g^{-1}, T is the temperature in K (*e.g.* 273 K, 293 K), a_i and b_j are the virial coefficients and m represents the number of coefficients required to adequately fit the isotherms (see section S2, ESI‡).

As an example, two SO_2 adsorption isotherms at 273 K and 293 K of NH_2-MIL-125(Ti) are shown in Fig. 6 and fitted with eqn (7).

A detailed description how to apply the virial fit in Origin for two isotherms simultaneously is given in the ESI‡ in the pdf slides. There is no general rule how many virial coefficients a_i and b_j should be used. In practice five a (a_0 to a_4) and two b parameters (b_0 and b_1) are good starting values for the fit. More parameters should be added until the final fit does not improve anymore. The quality of the fit can be evaluated by comparing R^2 and Chi^2 as well as by visual inspection.

In special cases a reasonable fit with the virial method is not possible. This is, for example, the case when a low uptake regime at the beginning of the isotherm is followed by stepwise uptake behavior with several inflection points in the micropore region as depicted in Fig. 7. We note that the standard linear (*n vs. p*) scale diagram of the adsorption isotherm (*cf.* Fig. S5 and S6, ESI‡) will not show such steps very well, whereas a logarithmic *p*-scale or double-logarithmic *n*- and *p*-scale will reveal such steps clearly. In such logarithmic-scale isotherm diagrams a better picture on the microporosity can be derived (Fig. S7 and S8, ESI‡).[32] The logarithmic scale of the absolute or relative pressure *p* yields step-like curves in the low-pressure region with the uptake steps related to the filling of pores of a certain size or adsorbent sites of a certain energy.

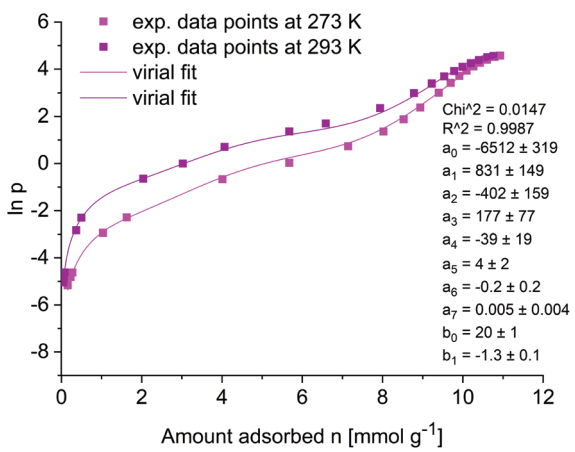

Fig. 6 Virial analysis for SO_2 adsorption isotherms of NH_2-MIL-125(Ti) at 273 K and 293 K with the fitting parameters (virial coefficients) a_i and b_j. The amount adsorbed n starts at 0.05 mmol g^{-1} (293 K) and 0.16 mmol g^{-1} (273 K) (see Fig. S5, ESI‡ for the usual *n vs. p* isotherm presentation). The virial coefficients a_i have the unit [K mol^{-i}]. Isotherm data taken from ref. 29.

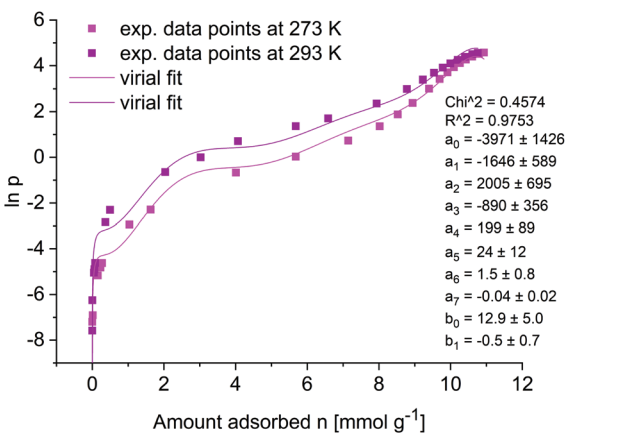

Fig. 7 Virial analysis for SO_2 adsorption isotherms of NH_2-MIL-125(Ti) at 273 K and 293 K with additional low uptake points, starting at n = 0.0002 mmol g^{-1} (see Fig. S6, ESI‡ for the usual *n vs. p* isotherm presentation). The virial coefficients a_i have the unit [K mol^{-i}]. Isotherm data taken from ref. 29.

The pressure ranges for these steps depend on the pore sizes or adsorption enthalpies. The linear (*n vs. p*) scale with the very steep uptake at very low pressures (p_{abs} < ~10 kPa or p/p_0 < ~0.1) for microporous materials cannot present any uptake steps as the larger pressure region from 10 < p_{abs} < 100 kPa takes up most (90%) of the axis length. The logarithmic scale, on the other hand, expands and presents at over 80% of the axis length the pressure region below 10 kPa. (We note that the fit problem of such uptake steps in the low-pressure region is in principle not limited to the virial fit but also applies to the Freundlich–Langmuir fit. It is just more apparent for the virial fit since it is based on the 'ln *p vs. n*' plot with the inherent expansion on the low-pressure region.)

The isotherms in Fig. 7 cannot be reliably fitted, even by adding more *a* and *b* parameters (see Fig. S9, ESI‡ for a fit of Fig. 7 with additional *a* and *b* parameters). Hence, the adsorption data points in the low pressure range had to be excluded to enable a reasonable fit as shown in Fig. 6. As a consequence, this implies that one cannot report a ΔH_{ads} for adsorptions below the range of the used and fitted gas uptake values.

From the virial fit, $\Delta H_{ads}(n)$ is then calculated by multiplying the ideal gas constant *R* with the sum of the a_i coefficients multiplied by the uptake *n* to the power of *i* (eqn (8)) (see the Excel sheet Ex3 (ESI‡) for computational details):

$$\Delta H_{ads}(n) = R \cdot \sum_{i=0}^{m} a_i n^i \quad (8)$$

(See eqn (S29) in ESI‡ for eqn (8) in the form $Q_{st} = -R\sum a_i n^i$ as it is normally given in the literature). Note that eqn (8) will yield a negative value for $\Delta H_{ads}(n)$ from the most important coefficient a_0 being negative. (Furthermore, with the unit of the ideal gas constant *R* of J K^{-1} mol^{-1} and *n* with the unit mol, the virial coefficients a_i must have the unit K mol^{-i} in order to derive at the unit of (k)J mol^{-1} for ΔH_{ads}.) The isosteric enthalpy of adsorption, $\Delta H_{ads}(n)$, derived from the virial fit shown in Fig. 6, is plotted against the amount adsorbed *n* in Fig. 8. The higher isosteric enthalpy of adsorption for SO_2 compared, for example, to CO_2 (*vide supra*) or H_2 (*vide infra*) can be explained by stronger interactions between the polar, permanently dipolar SO_2 molecule and functional groups within the structure of the MOF adsorbent. As expected, a decrease in the enthalpy of adsorption is seen with increased loading as the higher energy binding sites are occupied first. The enthalpy of adsorption for SO_2 at/near zero coverage, $\Delta H_{ads}(n)$ in the amino-functionalized MOF NH_2-MIL-125(Ti) exhibits a value of −53 kJ mol^{-1} (from eqn (8) with the lowest experimental uptake for both isotherms of *n* = 0.16 mmol g^{-1} and the a_i given in Fig. 6). Such a high enthalpy of adsorption for amine functionalized MOFs is in good agreement with the literature.[26] Besides functional groups at the linker, open metal sites in MOFs are predestined for high binding-energy interactions with molecules and can exhibit high "zero-coverage" enthalpies of adsorption.[33,34]

The enthalpy of adsorption at zero (rather very low) coverage $\left(\Delta H^0_{ads}\right)$ is well approximated by multiplication of the ideal gas constant *R* (8.314 J mol^{-1} K^{-1}) and the first virial coefficient a_0 (eqn (9)):

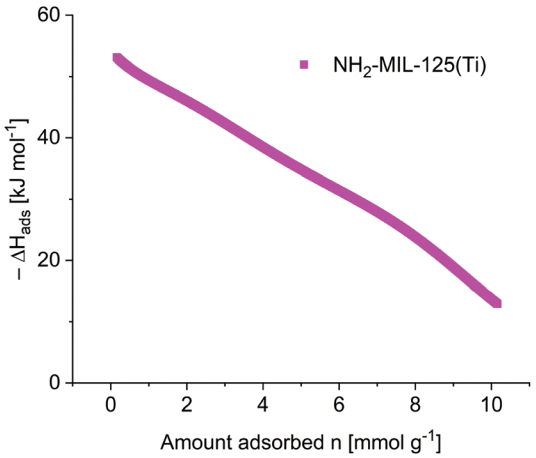

Fig. 8 Isosteric enthalpy of adsorption of SO_2 for NH_2-MIL-125(Ti) from a virial fit of the SO_2 adsorption isotherms at 273 K and 293 K in Fig. 6. The isotherms were fitted from n_{min} = 0.16 mmol g^{-1}. Computational details with eqn (8) are given in the Excel sheet Ex3 (ESI‡).

$$\Delta H^0_{ads} = R \cdot a_0 \quad (9)$$

(For very low coverage, $n \ll 1$, if *n* is set to 0, then the products $a_i\, n^i$ will all be 0, except for $a_0 \cdot 0^0 = a_0 \cdot 1$). At the same time, ΔH^0_{ads} is, however, strongly correlated with the value of the lowest coverage which is included in the virial analysis and is therefore heavily dependent on the measurement and calculation details. This is illustrated with the virial fits in Fig. 6 and 7. From Fig. 6 a_0 = −6511 K gives (with eqn (9)) $\Delta H^0_{ads} = -54$ kJ mol^{-1}, whereas from Fig. 7 a_0 = −3971 K yields $\Delta H^0_{ads} = -33$ kJ mol^{-1}. The value for a_0 is the most important of the polynomial coefficients. It is evident that a_0 can be adjusted with the uptake-pressure data points, which are included in the fit. Consequently, reports of record values for the enthalpy of adsorption at zero coverage, ΔH^0_{ads} should not be accepted without clear documentation how these values were derived. To judge the correctness of the virial fit it is mandatory to take the standard deviations of the coefficients into account. These standard deviations were given for the fits in Fig. 6 and 7. It is evident that the standard deviations for a_0 and a_1 for the (better) fit in Fig. 6 are significantly smaller than for the (worse) fit in Fig. 7. For a_0 in Fig. 6 the standard deviation is 5%, while for a_0 in Fig. 7 it is 36%. A too large standard deviation renders the fit value meaningless. It must be noted that we are not aware of standard deviations being discussed in virial fits of adsorption isotherms.

Clausius–Clapeyron *vs.* virial analysis

In this section a comparison between the Clausius–Clapeyron approach after Freundlich–Langmuir fitting and the virial analysis is presented for the calculation of the isosteric enthalpy

of adsorption. For the comparison we fitted H_2 adsorption isotherms at 77 K and 87 K on HHU-1 with a Freundlich–Langmuir approach and the virial analysis (Fig. 9) as described before. The goodness-of-isotherm fit in Fig. 9 top and bottom, judged visually and by R^2, seems to be similar for both methods (see also below). As a result, one would expect similar values for the isosteric enthalpy of adsorption. Nevertheless, $\Delta H_{ads}(n)$ calculated from both methods differs significantly as shown in Fig. 10. The most obvious difference in ΔH_{ads} between both models is present at close to zero coverage.

Usually in the literature,[35,36] and also here, the Clausius–Clapeyron approach with Freundlich–Langmuir-fitted isotherms shows a highly increased ΔH_{ads} at low amount adsorbed when compared to the virial analysis (Fig. 10). The accuracy of the Clausius–Clapeyron derived values is however questionable.[37] Enthalpies of adsorption derived from the virial analysis mostly exhibit smaller differences between low uptakes at zero coverage and bulk adsorption, which is considered more reasonable.[37]

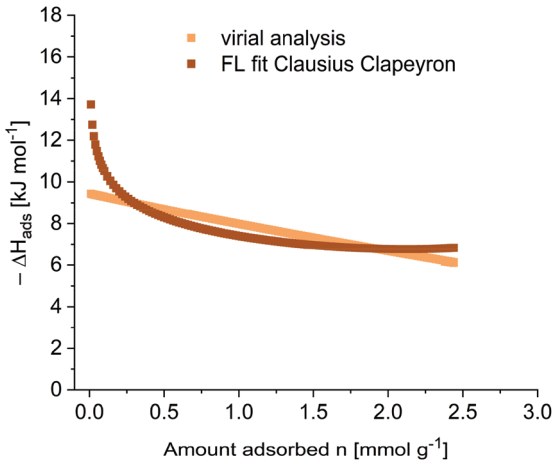

Fig. 10 $\Delta H_{ads}(n)$ calculated from H_2 adsorption isotherms on HHU-1 at 77 K and 87 K from virial analysis and a Freundlich–Langmuir fit together with the Clausius–Clapeyron equation. The isotherms were fitted from n_{min} = 0.01 mmol g^{-1} as lowest common experimental uptake for both isotherms.

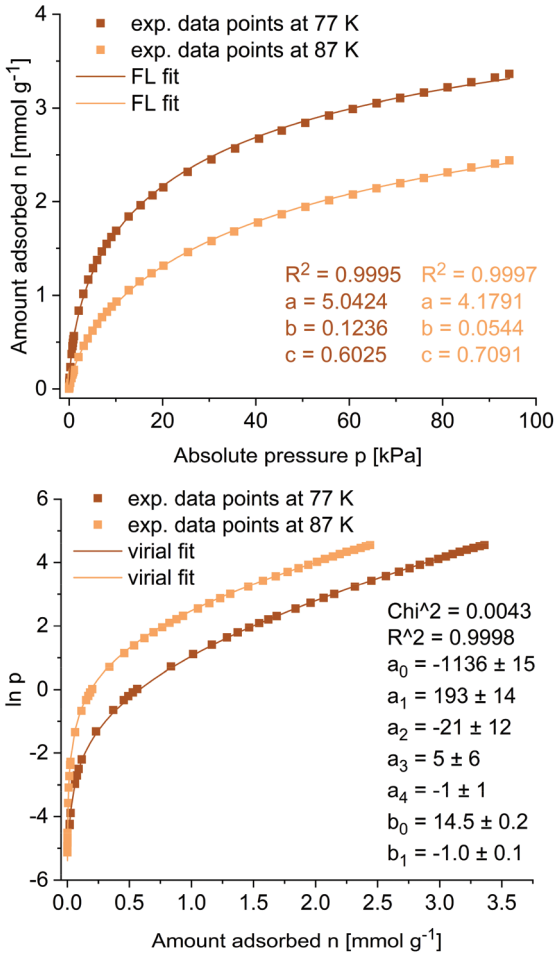

Fig. 9 Freundlich–Langmuir fit (top) and virial analysis (bottom) for H_2 adsorption isotherms on HHU-1 at 77 K and 87 K (see ESI‡ for structure details of HHU-1). The isotherms were fitted from n = 0.001 mmol g^{-1} (87 K) and n = 0.01 mmol g^{-1} (77 K). Computational details are given in the Excel sheet Ex4 (ESI‡). Note the small standard deviation for a_0 in the virial fit. The virial coefficients a_i have the unit [K mol^{-i}]. Isotherm data taken from ref. 38.

ΔH^0_{ads} for H_2 on HHU-1 derived from the Clausius–Clapeyron equation (−13.6 kJ mol^{-1}) is almost 1.5-fold higher than ΔH^0_{ads} calculated by virial analysis (−9.6 kJ mol^{-1}). Further, the Clausius–Clapeyron approach leads to an often-seen typical exponential-decay curvature with a high ΔH^0_{ads}, followed by a rapid decrease of the enthalpy of adsorption with increasing loading and an approach of a constant value at higher loadings. Yet, this constant ΔH_{ads} value of here ~−7 kJ mol^{-1} (Fig. 10) for the adsorption of H_2 on HHU-1 is still higher than the enthalpy of evaporation for H_2 (−0.9 kJ mol^{-1} at 20 K) which should be approached in the pore-filling regime with adsorptive–adsorbate interactions. To the contrary, ΔH_{ads} derived from virial analysis shows a moderate heat of adsorption at zero coverage and a rather linear decrease with increased loading.

This difference in $\Delta H_{ads}(n)$ from the Clausius–Clapeyron approach and the virial fit can be rationalized from a closer inspection of the goodness-of-fit at low amounts adsorbed. In the linear-scale n/p or $\ln p/n$ plots in Fig. 9 both fits seemed equally good. However, a logarithmic-scale n/p or $\ln p/n$ plot in Fig. 11 (for the same isotherms as in Fig. 9) reveals that the Freundlich–Langmuir fit for the Clausius–Clapeyron approach deviates significantly for loadings of n below ~0.1 mmol g^{-1}. On the other hand, the virial fit still covers almost all data points of n below ~0.1 mmol g^{-1}.

Yet, the isosteric enthalpies of adsorption from the Clausius–Clapeyron and virial approach are in general very similar, except for low loadings close to zero coverage and at (possible, but discouraged) extrapolation to (not measured) higher loadings (Fig. 10).

The Clausius–Clapeyron approach after Freundlich–Langmuir fitting can be improved by applying a dual-site

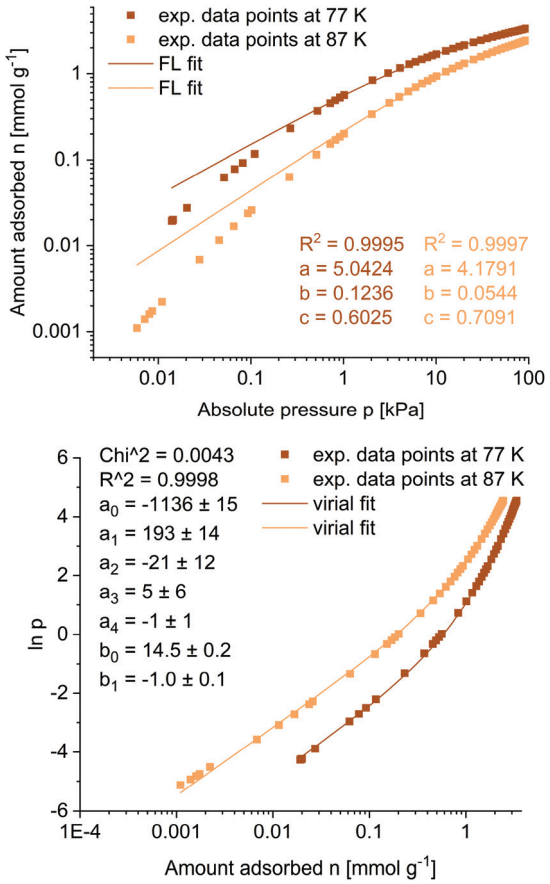

Fig. 11 Logarithmic-scale plots for Freundlich–Langmuir fit (top) and virial analysis (bottom) for H_2 adsorption isotherms on HHU-1 at 77 K and 87 K from Fig. 9.

Freundlich–Langmuir (DSFL) fit instead of the simpler Freundlich–Langmuir (FL) fit. Many isotherms cannot be suitably modeled by a single-site Langmuir or FL fit because multiple sites with different binding strengths are being occupied. Consistent with the previously used terms a dual-site Freundlich–Langmuir fit can be expressed as follows (eqn (10)):

$$n = \frac{a \cdot b \cdot p^c}{1 + b \cdot p^c} + \frac{a_1 \cdot b_1 \cdot p^{c_1}}{1 + b_1 \cdot p^{c_1}} \quad (10)$$

A dual-site approach is especially useful when determining isosteric enthalpies over a broad range, starting from "zero" loading. It is expected to find different adsorption enthalpies for varying loadings, due to different binding sites in the adsorbent. Thus, inclusion of a second or third site in the fitting model will then certainly yield a superior isotherm fit together with more reliable adsorption enthalpies derived therefrom. Fig. 12 depicts a comparison between the fits for a simple FL approach and the DSFL approach in a double logarithmic-scale n/p plot for H_2 in HHU-1 at 77 K and 87 K. For computational details see Excel sheet Ex4 and Origin file Or4, ESI.‡

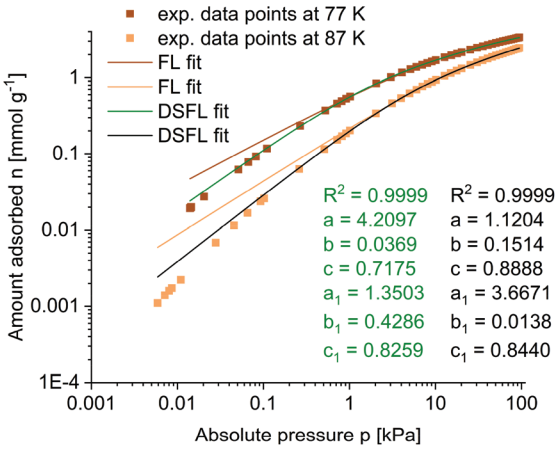

Fig. 12 Logarithmic-scale plots for Freundlich–Langmuir fits and dual-site Freundlich–Langmuir fits for the H_2 adsorption isotherms on HHU-1 at 77 K and 87 K from Fig. 9.

Visually and also judged by the goodness-of-fit, it is evident, that the DSFL fit approach is more reliable, especially at low uptakes at low pressures. This is in good agreement with the literature, where the DSFL approach gave superior fits compared to the FL approach or several other fitting models.[39,40] Concurrent with the improved fit, $\Delta H_{ads}(n)$ calculated from the Clausius–Clapeyron approach after DSFL fitting changes, compared to the FL fitting, as shown in Fig. 13.

The improved fitting data at low uptakes for the DSFL approach results in a much lower value for ΔH^0_{ads} of −10.5 kJ mol^{-1} compared to the value for ΔH^0_{ads} from the FL approach of −13.7 kJ mol^{-1}, while maintaining the characteristic and expected higher initial ΔH_{ads}. Also, at higher loadings ΔH_{ads} now does not remain constant but decreases, similar to the ΔH_{ads} calculated by virial analysis, and for n > ~1.2 the curva-

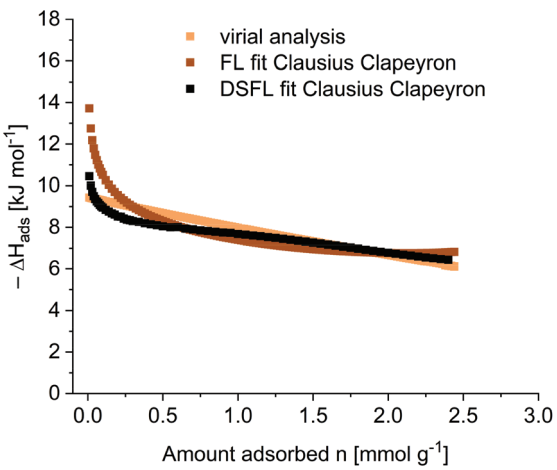

Fig. 13 $\Delta H_{ads}(n)$ calculated from H_2 adsorption isotherms on HHU-1 at 77 K and 87 K from virial analysis, FL fit and DSFL fit together with the Clausius–Clapeyron equation. The isotherms were fitted from n_{min} = 0.01 mmol g^{-1} as lowest common experimental uptake for both isotherms.

ture becomes nearly superimposable to the ΔH_{ads} curve from the virial analysis. Thereby, it is evident again that the FL fit can quite drastically overestimate ΔH^0_{ads}. Therefore, we encourage the reader to evaluate the Freundlich–Langmuir fit of their isotherms with a double logarithmic-scale *n vs. p* plot and if necessary apply a dual-site Freundlich–Langmuir fit. Still, when looking at the "improvement" in ΔH^0_{ads} from the FL to the DSFL fit (Fig. 13) and the remaining deviation between the DSFL fit and the experimental isotherms (Fig. 12) it can be assumed that even the DSFL fit somewhat overestimates the ΔH^0_{ads} value.

To conclude which approach is closer to the real values a comprehensive study with experimental data from calorimetric measurements compared to both methods would be needed. The enthalpy of adsorption can be directly obtained from calorimetric measurements, which is seldom done, however. So far, only very few calorimetric experiments are available for the enthalpy of adsorption of adsorbates for MOFs.[22] To the best of our knowledge we are not aware of calorimetric heat of adsorption values for which at the same time $\Delta H_{ads}(n)$ from both the Clausius–Clapeyron approach and the virial fit were derived.

For the open-metal-site MOF MIL-100(Cr) the enthalpy of adsorption for CO_2 was determined by microcalorimetry,[41] and calculated from adsorption isotherms at 273, 298 and 323 K with a Freundlich–Langmuir fit and Clausius–Clapeyron approach (Fig. S10, ESI‡).[42] A close comparison of both curves shows that the ΔH_{ads} values for low coverage match but the values deviate considerably with increasing loading. The empirical values from the isotherm fit lie substantially below the microcalorimetry values (Fig. S10, ESI‡). For the MOF HKUST-1 calorimetry and isotherm-fit values (Clausius–Clapeyron) match for low coverage; calorimetry values for higher coverage were not available.[23]

Conclusions

The good quality measurement of two or better three adsorption isotherms at different but close temperatures is a convenient way to derive the isosteric enthalpy of adsorption, ΔH_{ads} as a function of coverage (amount adsorbed), $\Delta H_{ads}(n)$. To be able to obtain reasonable enthalpies at zero coverage, ΔH^0_{ads} the experimental sorption analyzer should be able to operate in low-pressure regimes ($p/p_0 < 0.001$, or $p_{absolute} < 1.0$ mbar) in order to record low-uptake data points. The curve fits of experimental sorption isotherms must not be extrapolated below or above the measured data points, that is, any extrapolation from the isotherm fit is strongly discouraged. The thus determined zero-coverage enthalpy of adsorption, is directly associated with the lowest measured uptake data point. The fitting procedure of the isotherms is of major importance for $\Delta H_{ads}(n)$.

The virial analysis can be superior over the Freundlich–Langmuir fit/Clausius–Clapeyron approach in order to obtain rational ΔH^0_{ads} values, as the Freundlich–Langmuir fit may deviate strongly for low-uptake data points, which should always be checked in a logarithmic-scale *n vs. p* plot. If a large deviation is apparent, a dual-site Freundlich–Langmuir fit should be applied to improve the fit. When the goodness-of-fit for the dual-site approach (especially at low uptakes of the logarithmic-scale *n vs. p* plot) becomes sufficient, the Clausius–Clapeyron approach to obtain ΔH^0_{ads} values has a certain merit, since physically meaningful parameters are used in the equation, whereas the virial expression is completely empirical.

For a virial fit it is mandatory to ensure low standard deviations of the obtained virial coefficients. In general, the derived isosteric enthalpy of adsorption is only as accurate as the recorded isotherm and the applied fit.

Glossary (alphabetic)

Absorption. The term absorption is used, when the species of the adsorptive penetrate the surface layer and enter the dense (not porous) structure of the bulk solid.

Adsorption and desorption. Physical adsorption, physisorption or in short simply adsorption is the enrichment or adhesion of species from a gas or liquid phase at a solid surface, that is at a solid–gaseous or solid–liquid interface. Desorption is the opposite process of removing the adsorbed species from the surface. The surface is part of the adsorbent; the adsorbed species form the adsorbate (Fig. 14). The forces responsible for adsorbate–adsorbent interactions in physical adsorption start from weak van-der-Waals forces for non-polar gases (solutes) such as Ar and the other noble gases. Other physisorbed species can exert additional attractive forces such as quadrupole–quadrupole (*e.g.* N_2, CO_2, H_2), dipole–dipole (*e.g.* SO_2) or hydrogen bonding interactions (*e.g.* H_2O, NH_3). Finally, chemical adsorption, that is, chemisorption leads to stronger chemical bonds (ionic, covalent, coordinative) between the adsorbed species and the surface (Fig. 15). The maximum possible amount of an adsorbate at a surface is

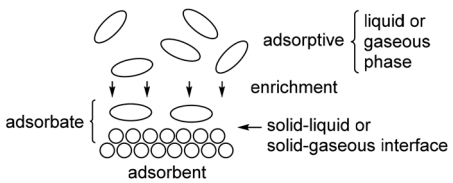

Fig. 14 Schematic illustration of an adsorption process of a gaseous or liquid phase on a solid surface.

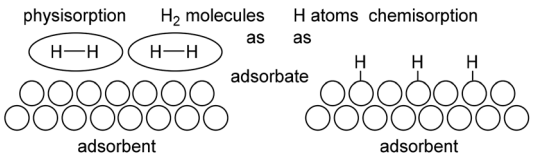

Fig. 15 Illustration of the difference between physi- and chemisorption for the case of the adsorptive H_2.

given by the (accessible) surface area of the adsorbent. For systems close to saturation adsorption should be viewed as a pore-filling process rather than adsorbate monolayer formation. Gas (solute) uptake capacity under these saturation conditions is eventually governed by pore volume and not by the surface area or strength of adsorbent–adsorbate interaction. The adsorbed amount is usually based on a unit mass, *e.g.* 1 gram, of adsorbent, so that the sorption capacities of different materials can be compared.

Adsorbate refers to a two-component system, consisting of the solid adsorbent and the adsorbed molecules (Fig. 14). Often adsorbate is used to mean only the adsorbed species.

Adsorbent is the solid phase with external or internal surface, which is exposed to the gaseous or liquid molecules (Fig. 14).

Adsorptive are the free gaseous or solute molecules, which have not yet been adsorbed onto the surface (Fig. 14).

Chemisorption and physisorption. Depending on the interaction strength or binding energy by which molecules are bound onto a surface, one can differentiate between chemisorption or physisorption phenomena. Physisorption is a reversible physical adsorption with low binding energies *via* van-der-Waals forces (Fig. 15). The adsorption is strongly temperature-dependent, not specific, can form multilayers and shows low enthalpies ("heat") of adsorption. In chemisorption molecules are bound to the surface of the solid by strong "chemical" bonds (ionic, covalent, coordinative and also strong hydrogen bonds) with high enthalpies of adsorption. There is only the formation of a single adsorption layer (monolayer), which occurs less independent of temperature. Chemisorption is specific to the surface characteristics of the adsorbent. An example for chemisorption is the dissociative binding of the adsorptive H_2 as a metal hydride (Fig. 15).

Desorption. See Adsorption.

Freundlich isotherm. The Freundlich adsorption isotherm is an empirical expression for the quantity of gas (or solute) adsorbed by a solid adsorbent at different pressures:

$$\frac{x}{m} = a \cdot c^{\frac{1}{n}}$$

where x is the mass of the adsorbed species, m is the mass of the adsorbent, c is the equilibrium concentration of adsorbate in solution and a, n are substance and temperature specific constants (here n is not to be mistaken with the amount adsorbed or loading n). Due to its exponential nature the Freundlich adsorption isotherm is not valid for high loadings.

Isoster means (here) the same surface coverage, which is equivalent to the same gas uptake or loading (n). When the heat of adsorption, ΔH_{ads} is calculated as the **isosteric** heat of adsorption, it refers to the same surface coverage, when determined from two adsorption isotherms at two different temperatures.[16]

Isotherms are lines with the same temperature in, *e.g.*, a p–V (pressure *vs.* volume) or a p–n (pressure *versus* uptake) diagram. In adsorption studies p–n diagrams are measured and evaluated for surface area and porosity. An isotherm assumes thermodynamic equilibrium between the adsorptive/adsorbate and adsorbent at each $p|n$ data point. The shape and hysteresis for the adsorption and desorption isotherm can be already used to classify materials as micro–meso–macroporous and also with respect to pore shape.[16]

Enthalpy of adsorption, ΔH_{ads} is defined as the heat to be released when an adsorptive physisorbs to the surface of the adsorbent. For physisorption the enthalpy of adsorption is the reverse of the enthalpy of desorption, ΔH_{des}, which is required for the reverse process to detach an adsorbate ($\Delta H_{ads} = -\Delta H_{des}$).

Langmuir isotherm. The Langmuir adsorption isotherm is an empirical expression for the quantity of gas (or solute) adsorbed and is based on three main assumptions for the gas–solid interaction: (i) solely single adsorption layer (monolayer) formation, (ii) a homogenous surface, (iii) without interactions of adsorbates on neighboring adsorption sites.

$$\frac{x}{m} = \frac{a \cdot c}{1 + b \cdot c}$$

where x is the mass of the adsorbed species, m is the mass of the adsorbent, c is the equilibrium concentration of adsorbate in the gas or solution phase, a is the maximal loading of the adsorbate and b is the Langmuir constant.

Porosity refers to the free volume or empty space in a porous material in relation to its total volume. Micro- and meso-porosity is typically probed by gas sorption under isothermal conditions, *e.g.*, N_2 gas sorption measurements at 77 K which yields n–p gas sorption isotherms. For each data point a thermodynamic equilibrium between the adsorptive/adsorbate and adsorbent is assumed. The isotherms are usually evaluated by the Brunauer–Emmett–Teller (BET) method for the accessible specific surface area (in $m^2\ g^{-1}$) and/or specific pore volume (in $cm^3\ g^{-1}$). For microporous materials the BET surface area is more precisely referred to as 'apparent BET' area. The BET-area derived from a Type I isotherm (which is characteristic for microporous materials) must not be treated as a realistic probe accessible surface area. It represents an apparent surface area, which may be regarded as a useful adsorbent "fingerprint". For microporous materials surface area and pore volume can be identical for a range of small micropores and pore blocking can more easily occur.

Additional (so called Rouqueroul) criteria need to be fulfilled when determining the capacity for microporous materials. For more details, we refer to the latest IUPAC report of physisorption of gases from 2015.[16] Alternatively, Ar (at 87 K), Kr (at 77 K) or CO_2 (between 195 K to ambient temperature) can be used to probe micro- and mesopores. The term "specific" means that the surface area values are based on (referenced to) a unit mass, *e.g.* 1 gram, of the adsorbent. The pore size is defined as (i) micropores with diameters <2 nm, (ii) mesopores with diameters between 2–50 nm, (iii) macropores with diameters exceeding (>) 50 nm.

Pore structures of porous materials can be diverse and consist of different pore sizes and shapes with, *e.g.*, larger cavities and smaller pore windows, which complicates their characterization. Further, the accessibility of pores is only

possible if the kinetic diameter of the adsorptive is smaller than the pore or pore window diameter, otherwise the potentially available pores are blocked for this specific adsorptive.

Sorption. If it is not possible to distinguish between absorption and adsorption it is convenient to use the more general term sorption which includes both phenomena. Then one should also use the derived terms sorbent, sorbate and sorptive accordingly (*cf.* Fig. 14).

Surface coverage is defined as the number of occupied adsorption sites dived by the number of available adsorption sites. Adsorption sites can further be divided into internal and external surface area. The external surface area describes adsorption on the outside of particles, while internal surface area means the surface of all inner pore walls.

Conflicts of interest

There are no conflicts to declare.

Acknowledgements

We thank Mr Philipp Brandt and Dr Jun Liang for reading the manuscript and for valuable suggestions and the Referees for their helpful and constructive comments.

References

1 R. Batten, N. R. Champness, X.-M. Chen, J. Garcia-Martinez, S. Kitagawa, L. Öhrström, M. O'Keeffe, M. P. Suh and J. Reedijk, *Pure Appl. Chem.*, 2013, **85**, 1715–1724.
2 A. Kirchon, L. Feng, H. F. Drake, E. A. Joseph and H.-C. Zhou, *Chem. Soc. Rev.*, 2018, **47**, 8611–8638.
3 A. E. Baumann, D. A. Bruns, B. Liu and V. S. Thoi, *Commun. Chem.*, 2019, **2**, 86.
4 H. Li, K. Wang, Y. Sun, C. T. Lollar, J. Li and H.-C. Zhou, *Mater. Today*, 2018, **21**, 108–121.
5 B. Li, H.-M. Wen, W. Zhou and B. Chen, *J. Phys. Chem. Lett.*, 2014, **5**, 3468–3479.
6 K. Sumida, D. L. Rogow, J. A. Mason, T. M. McDonald, E. D. Bloch, Z. R. Herm, T.-H. Bae and J. R. Long, *Chem. Rev.*, 2012, **112**, 724–781.
7 J. Liu, P. K. Thallapally, B. P. McGrail, D. R. Brown and J. Liu, *Chem. Soc. Rev.*, 2012, **41**, 2308–2322.
8 A. Ahmed, S. Seth, J. Purewal, A. G. Wong-Foy, M. Veenstra, A. J. Matzger and D. J. Siegel, *Nat. Commun.*, 2019, **10**, 1568–1577.
9 M. P. Suh, H. J. Park, T. K. Prasad and D.-W. Lim, *Chem. Rev.*, 2012, **112**, 782–835.
10 K. Sumida, C. M. Brown, Z. R. Herm, S. Chavan, S. Bordiga and J. R. Long, *Chem. Commun.*, 2011, **47**, 1157–1159.
11 S. K. Bhatia and A. L. Myers, *Langmuir*, 2006, **22**, 1688–1700.
12 J. M. Crow, *ChemistryWorld*, 2019, September, pp. 48–52.
13 Y. He, W. Zhou, G. Quian and B. Chen, *Chem. Soc. Rev.*, 2014, **43**, 5657–5678.
14 X. Han, S. Yang and M. Schröder, *Nat. Rev. Chem.*, 2019, **3**, 108–118.
15 S. Sircar, *Adsorpt. Sci. Technol.*, 2001, **19**, 347–366.
16 M. Thommes, K. Kaneko, A. V. Neimark, J. P. Olivier, F. Rodriguez-Reinso, J. Rouquerol and K. S. W. Sing, *Pure Appl. Chem.*, 2015, **87**, 1051–1069.
17 D. Nicholson and T. Stubos, Recent Advances in Gas Separation by Microporous Ceramic Membranes, in *Membrane Science and Technology*, Elsevier, 2000.
18 J. Rouquerol, F. Rouquerol and K. S. W. Sing, *Adsorption by powders and porous solids*, Academic Press, San Diego, USA, 1999.
19 S. Sircar and D. V. Cao, *Chem. Eng. Technol.*, 2002, **10**, 945–948.
20 S. Keskin, T. M. van Heest and D. S. Scholl, *ChemSusChem*, 2010, **3**, 879–891.
21 H. W. Langmi, J. Ren, B. North, M. Mathe and D. Bessarabov, *Electrochim. Acta*, 2014, **128**, 368–392.
22 Z. Du, X. Nie, S. Deng, L. Zhao, S. Li, Y. Zhang and J. Zhao, *Microporous Mesoporous Mater.*, 2020, **298**, 110053.
23 D. Farrusseng, C. Daniel, C. Gaudillere, U. Ravon, Y. Schuurman, C. Mirodatos, D. Dubbeldam, H. Frost and R. Snurr, *Langmuir*, 2009, **25**, 7383–7388.
24 (*a*) J. Tóth, *Adv. Colloid Interface Sci.*, 1995, **55**, 1–239; (*b*) K. V. Kumar, S. Gadipelli, B. Wood, K. A. Ramisetty, A. A. Stewart, C. A. Howard, D. J. L. Brett and F. Rodriguez-Reinoso, *J. Mater. Chem. A*, 2019, **7**, 10104–10137.
25 H. Pan, J. A. Ritter and P. B. Balbuena, *Langmuir*, 1998, **14**, 6323–6327.
26 S. Yang, J. Sun, A. J. Ramirez-Cuesta, S. K. Callear, W. I. F. David, D. P. Anderson, R. Newby, A. J. Blake, J. E. Parker, C. C. Tang and M. Schröder, *Nat. Chem.*, 2012, **4**, 887–894.
27 J. H. Carter, X. Huan, F. Y. Moreau, I. da Silva, A. Nevin, H. G. W. Godfrey, C. C. Tang, S. Yang and M. Schröder, *J. Am. Chem. Soc.*, 2018, **140**, 15564–15567.
28 A. G. Bezus, A. V. Kiselev, Z. Sedlacek and P. Q. Du, *Trans. Faraday Soc.*, 1971, **67**, 468–482.
29 P. Brandt, A. Nuhnen, M. Lange, J. Möllmer, O. Weingart and C. Janiak, *ACS Appl. Mater. Interfaces*, 2019, **11**, 17350–17358.
30 *Origin(Pro)*, Version Number, 2019, 9.6.0.172, OriginLab Corporation, Northampton, MA, USA.
31 D. Ma, J. Zhang, J. Bai and H. Zhang, *Nat. Res.*, 2014, **5**, 782–794.
32 N. Maes, H.-Y. Zhu and E. F. Vansant, *J. Porous Mater.*, 1995, **2**, 97–105.
33 Ü. Kökcam-Demir, A. Goldman, L. Esrafili, M. Gharib, A. Morsali, O. Weingart and C. Janiak, *Chem. Soc. Rev.*, 2020, **49**, 2751–2798.
34 Z. Zhang, Y. Zhao, Q. Gong, Z. Li and J. Li, *Chem. Commun.*, 2013, **49**, 653–661.
35 Z. Zhao, Z. Li and Y. S. Lin, *Ind. Eng. Chem. Res.*, 2009, **48**, 10015–10020.
36 S. R. Caskey, A. G. Wong-Foy and A. J. Matzger, *J. Am. Chem. Soc.*, 2008, **130**, 10870–10871.

37 J. L. C. Rowsell and O. M. Yaghi, *J. Am. Chem. Soc.*, 2006, **128**, 1304–1315.
38 T. J. Matemb Ma Ntep, H. Reinsch, B. Moll, E. Hastürk, S. Gökpinar, H. Breitzke, C. Schlüsener, L. Schmolke, G. Buntkowsky and C. Janiak, *Chem. – Eur. J.*, 2018, **24**, 14048–14053.
39 F. V. A. Dutra, B. C. Pires, T. A. Nascimento, V. Mano and K. B. Borges, *RSC Adv.*, 2017, **7**, 12639–12649.
40 S. J. Caldwell, B. Al-Duri, N. Sun, C. Sun, C. E. Snape, K. Li and J. Wood, *Energy Fuels*, 2015, **29**, 3796–3807.
41 P. L. Llewellyn, S. Bourrelly, C. Serre, A. Vimont, M. Daturi, L. Hamon, G. De Weireld, J. S. Chang, D. Y. Hong, Y. K. Hwang, S. H. Jhung and G. Férey, *Langmuir*, 2008, **24**, 7245–7250.
42 J. Yang, H. Bai, F. Zhang, J. Liu, J. Winarta, Y. Wang and B. Mu, *J. Chem. Eng. Data*, 2019, **64**, 5814–5823.